International Journal of Hydrogen Energy 58 (2024) 28–39

Contents lists available at ScienceDirect

International Journal of Hydrogen Energy

journal homepage: www.elsevier.com/locate/he

An experimental study on $H_2/NH_3/CH_4$-air laminar propagating spherical flames at elevated pressure and oxygen enrichment

Ahmed Yasiry [a,b], Jinhua Wang [a], Longkai Zhang [a], Ahmed A.A. Abdulraheem [c], Xiao Cai [a,*], Zuohua Huang [a]

[a] State Key Laboratory of Multiphase Flow in Power Engineering, Xi'an Jiaotong University, Xi'an, 710049, China
[b] Automotive Engineering Department, College of Engineering-Musaib, University of Babylon, Babil, 51002, Iraq
[c] Mechanical Engineering Department, College of Engineering, University of Babylon, Babil, 51002, Iraq

ARTICLE INFO

Keywords:
Ternary fuel
$H_2/NH_3/CH_4$
Constant volume chamber
Laminar flame speed

ABSTRACT

This study measures the accurate Laminar Burning Velocities (LBVs) of ($H_2/NH_3/CH_4$) ternary fuels-air flames under elevated pressure and oxygen enrichment using a constant volume chamber, providing reliable experimental data to verify the detailed chemical kinetic mechanism. Results show that the LBV values for blending ratios of H_2/NH_3 of 10%–50% demonstrate a suitable alternative energy-generated fuel for conventional fuels in industrial applications, and the maximum value of LBV is achieved at an equivalence ratio close to 1.05. Increasing H_2 blends will increase LBV non-linearly under any conditions and decrease with an increase in ammonia blends. Increasing the initial pressure decreases LBV; at 10% H_2, LBV decreases by 33% at 0.3 MPa and 45% at 0.5 MPa compared to atmospheric pressure. Furthermore, increasing oxygen content improves the reactivity of the mixture and accelerates LBV due to increasing the OH, NH_2, and CH_3 radicals. Maintaining a constant value of LBV requires controlling the blending ratio of the ternary fuels, where increasing LBV values shift the blending of the mixture towards higher hydrogen and methane concentrations and fewer ammonia concentrations. Finally, the effect of maintaining a constant value of adiabatic flame temperature and density ratio on flame characteristics is explained, making the selection of an alternative ternary blending fuel more precise.

1. Introduction

With the diversification of renewable energy sources, the electrification of automobiles, and developments in fuel cell technologies have raised questions about the future of traditional energy systems such as internal combustion engines and gas turbines. These systems are expected to remain prevalent due to their high energy density and cost-effective fuel distribution. However, the urgent need to address global warming, fossil fuel shortages, and air pollution has increased the importance of integrating renewable, low-carbon, or carbon-free fuels into power and energy systems to enhance efficiency, reduce emissions, and optimize engine performance. Hydrogen (H_2) and ammonia (NH_3) have been proposed as a form of renewable and clean energy and an energy carrier to store and transport intermittent renewable energy sources, such as solar photovoltaics and wind, over a long distance at a significantly lower cost than liquefied H_2 [1]. The recent development in the fundamental study of ammonia combustion to develop cleaner and more cost-effective hydrogen storage and transportation has resulted from the intense trend in applying ammonia as a hydrogen energy carrier and a carbon-free fuel. Reviews in the literature provide an overview of the existing advances in ammonia applications, particularly in the field of the most recent knowledge of ammonia combustion [1–5].

Table 1 indicates that hydrogen has the highest laminar burning velocity with extended flammability limits and low minimum ignition energy, while ammonia has not been considered a fuel due to its lower adiabatic flame temperature, high minimum ignition energy and nitrogen atom in its molecule, narrower flammability limits [6], and lower laminar burning velocity [7], hence low heat release rate with poor flame stabilization characteristics, low combustion efficiency [8,9]. However, ammonia is not only a suitable hydrogen carrier made up of 17.8% by weight of hydrogen, but it also offers a higher hydrogen density (121 kg–H_2/m^3) than liquid hydrogen (70.8 kg–H_2/m^3), which makes it a feasible alternative since more hydrogen can be obtained [10]. Hydrogen requires a very low temperature (−252.9 °C) to liquefy compared with ammonia (−33.4 °C) at ambient pressure; hydrogen can also be liquefied at room temperature with high pressure

* Corresponding author.
E-mail address: xiao.cai@xjtu.edu.cn (X. Cai).

https://doi.org/10.1016/j.ijhydene.2024.01.138
Received 14 November 2023; Received in revised form 23 December 2023; Accepted 12 January 2024

Table 1
Fundamental combustion characteristics and thermal properties of ammonia, hydrogen, and methane fuels [1].

Property	NH_3	H_2	CH_4
Boiling temperature at 0.1 MPa	−33.4	−252.9	−161
Lower heating value (MJ/kg)	18.6	120	50.0
Flammability limit (Lower ϕ)	0.63	0.10	0.50
Flammability limit (Higher ϕ)	1.40	7.1	1.7
Adiabatic flame temperature (K)[a]	1800	2110	1950
Maximum LBV (m/s)[b]	0.07	2.91	0.37
Auto ignition temperature	650	520	630

[a] Property measured at $\phi = 1$.
[b] Maximum LBV occurs at different ϕ.

(350–700 bar) compared with ammonia of (8.5 bar) [11]. Due to these advantages, ammonia represents a potentially valuable CO_2 - free fuel in fuel cells [12,13], gas turbines [14,15], boilers or internal combustion engines [16,17].

Laminar burning velocity (S_L) is a physiochemical parameter that defines the movement of reactant mixture to the reaction zone, including the mixing and reaction to represent the fundamental combustion, reproducing the diffusion, exothermicity, and reactivity of the fuel mixtures [18]. In addition to outlining laminar and turbulent premixed characteristics concurrently inside the laminar flamelet regime, measuring accurate laminar burning velocity is an important evaluative aspect in progressing the comprehension of a wide range of flames and flame stabilization, validating the chemical kinetics of the fuel and its combustion characteristics [19,20].

Several research reviewed extensively laminar burning velocity (LBV) of hydrogen [21], ammonia [3], and methane [22] flames, implementing the effects of different equivalence ratios [23–25], initial pressures [26–28], and initial temperatures [29,30]. In addition, many chemical kinetic models of oxidation and pyrolysis have been presented and tested, providing effective conclusions for predicting the laminar burning velocity of hydrogen [31,32], ammonia [33,34], and methane [35,36] flames.

Researchers have extensively studied the effect of dual fuel blending because fuels are often a mixture of many chemical components, and it is useful to be able to guess the laminar burning velocity of a mixture of two or more components using the laminar burning velocity for each single fuel. Using the volume [37] or mass [38] fraction method as the simplest mixing rule to estimate the laminar burning velocity. Besides, researchers also investigated different correlations to predict LBV [38–40]. The hydrogen addition improved overall reactivity due to the addition of extinction strain rate increases by 2.5–3.8 times and 2 to 3 times by increasing only 1%–5% and 4% H_2 in the fuel mixture, respectively [41], while 1.5–2 times increase in H and OH radical peaks with 50% addition of H_2 in the biogas for laminar premixed flames [42].

Mashruk et al. [43] examined the combustion characteristics of ternary fuel in a generic tangential swirl burner at constant power (8 kW), equivalence ratio (1.2), and blending ratios of 10, 20, and 30% (vol)H_2. It showed that increasing the concentration of ammonia affects operability; also, high ammonia blends convert from OH/CH/NH formation to NH_2. Hydrogen addition enhances operability by up to 30% (vol) when added. With no evident flashback, reduced emissions, low carbon content, and reasonable production of NH_2/OH radicals for excellent operability, the (20) methane/(55) ammonia/(25) hydrogen (% vol) blend seems to be the most promising.

Benaissa et al. [44] investigated the combustion characteristics and emissions of biogas/hydrogen blends in a can-type gas turbine (SIEMENS SGT750) Combustor of 60 kW using the non-premixed flamelet model, P-1 radiation model and turbulent standard (k–ϵ) model. It can be noticed that increasing the hydrogen blend reinforced the reaction zone and enhanced the emissions and the stabilization of the flame. Comparing biogas with 50% H_2, a maximum NO emissions reduction can be found by 43 and 78 (ppm @15% by volume of O_2), respectively. The flame temperature and NO emissions at $\phi = 0.2$ with a high rate of hydrogen (50% H_2) are close to the results of pure biogas (0% H_2) at the same ϕ. Additionally, CO and CO_2 emissions decreased with increasing H_2 blend and decreasing the ϕ; due to an increase in OH concentration and a decrease in carbon concentration.

Berwal et al. [30] examined the laminar burning velocity of XNH_3 + $0.8(1–X)CH_4$ + $0.2(1–X)H_2$-air flames where X = (0%–30% vol) using the externally heated diverging channel technique at high initial temperatures (300 K–750 K). LBV increased with the initial temperature and decreased with ammonia blending. The Nitroxyl (HNO) radical caused a 28% reduction with 30% NH_3. Berwal et al. [45,46] also investigated the ammonia blending effect on the LBV of methane/hydrogen premixed flames at elevated temperature and pressure conditions utilizing the high-pressure diverging-channel method. It demonstrated the viability of ternary fuel as a good alternative to reduce carbon emissions by about 26.6% when ammonia increases by 30%. The temperature exponent, α, does not change when the ammonia blends and minimum value at $\phi = 1.1$ at elevated pressure, while the pressure exponent, β, increases with increasing initial temperatures.

Bayramoğlu et al. [47] investigated the $H_2/NH_3/CH_4$ fuel blends numerically on the combustion emissions and performance for 5%–10%–15% hydrogen blend with methane as a binary blending fuel. Furthermore, a fixed 5% hydrogen with 5%–10%–15% ammonia blends with methane as a ternary blending fuel, where the results showed that at an axial location of x/d = 0.444, NOx emission production increased by 1970, 3010, and 3790 ppm, respectively. 15% hydrogen and ammonia blends added to methane increase the maximum temperature by 100 and 200 K, respectively. Moreover, CO_2 reduction compared to neat methane (100% methane) by 30.7% and 14%, respectively. Regarding emission production, pure ammonia performs better NO than ammonia–hydrogen and methane–ammonia dual fuel blends at any blending ratio. This feature agrees with the literature [48–52]. Increasing ammonia blending decreases Tad, which leads to decreased thermal NO production [50], which still accounts for a fraction of the total NO production [51]. Maximum NO concentrations are found to slightly lean due to the large OH and O mole fraction at a higher temperature that contributes to NO formation via fuel NOx pathways [48]. While for very lean or rich ($\phi \geq 1.10$) equivalence ratios, a lower value of NO mole fractions (<100 ppm) is found. The availability of NH2 radicals increases with increases ϕ towards stoichiometric and rich, which promotes the reaction $NH_2 + NO \rightarrow H_2O + N_2$, which consumes NO. Nevertheless, regarding ammonia methane combustion, the HCN plays a great role in NO formation via fuel NOx pathways. The same trend of increasing NO formation towards $\phi = 0.8$ due to OH and O radicles and then starts to decrease due to NH_2 radicle [52]. Tang et al. [53] investigated ammonia's premixed combustion limits of hydrogen and methane additives. They proved low values of lower blow-out and lean combustion limits while high values of rich combustion limits for NH_3-H_2 flames. When hydrogen is added to the ammonia combustion process, the adiabatic flame temperature increases and it can lead to more complete and efficient combustion, reducing the formation of NOx. This is because hydrogen has a high flame speed and can enhance combustion, lowering overall emissions. Additionally, using appropriate catalysts and combustion processes can further help reduce NOx emissions when using a hydrogen–ammonia blend as a fuel. Moreover, increasing H_2 blends improves the overall reactivity and fuel consumption rate due to increased hydroxyl oxidation reaction rate. The results also showed that LBV of the ternary mixture is close to natural gas/methane results with 10% CO- CO_2 reduction, especially for higher temperatures (>550 K) for lean and stoichiometric conditions, and increasing X_{NH_3} decreases CO/CO_2 emissions. Hence, it can be used as a clean fuel with low carbon emissions for engine applications.

The motivation for this study will support the research area with a proposal of an alternative ternary blended fuel with equivalent laminar burning velocity and low carbon emissions as compared to natural gas

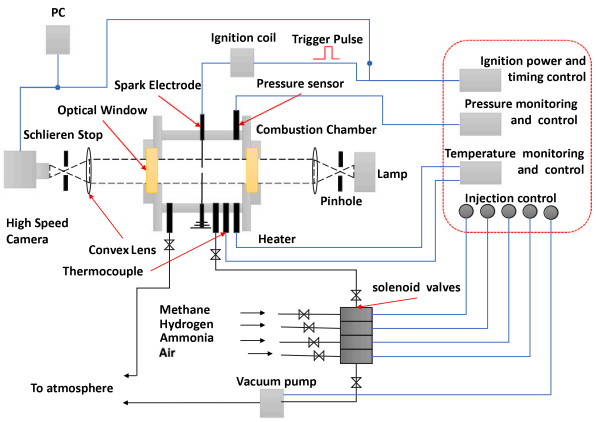

Fig. 1. Schematic of the experimental setup.

to be mimicked. This work aims to investigate the laminar burning velocity at different blending ratios, initial pressure, oxygen enrichment, and equivalence ratios. Experiments are performed to examine the laminar burning velocity under the selection of blending ratios based on constant adiabatic flame temperature, and density ratios for ternary fuel. In addition to a mixture of binary fuels of hydrogen–ammonia and ammonia–methane–air mixtures and (0%–40%) hydrogen–ammonia–methane–air mixtures at an initial pressure of (0.1–0.5 MPa), and oxygen enrichment (21, 35 and 45%), and equivalence ratios ranging from 0.8 to 1.2 at a temperature of (298 K). This study examines the use of hydrogen and ammonia-based combustion, so the framework of this study is structured as follows: Section 1 presents an introduction to this study. Section 2 presents the experimental setup and procedure. The Section 3 presents laminar flame measurements for binary and ternary fuel and sensitivity analyses. The section of 4 summarizes the study's conclusion.

2. Experimental setup and methodology

Experiments were conducted on a specially fabricated high-pressure constant volume combustion chamber at the Department of Mechanical Engineering, the University of Babylon in Iraq. Fig. 1 shows a schematic diagram of the experimental setup. The second chamber was used to conduct high-pressure experiments conducted at Xi'an Jiaotong University's State Key Laboratory of Multiphase Flow in Power Engineering — China. The laminar flame speed at different equivalence ratios, blending ratios, initial pressure, and oxygen ratios are measured directly. The volume of the chambers is (29 and 23.5) L, with an inner length of (400 and 310) mm, respectively, and an inner diameter of 305 mm for both chambers. Two electrodes with a spark gap of 1.5 mm and a diameter of 1 mm are symmetrically positioned on the chamber wall to ignite the gas mixture. Two equal quartz windows for each chamber with an optical diameter of (120 and 150) mm, respectively, were positioned opposite each other to allow for visualizing the laminar spherically expanding flames using the Schlieren method with a high-speed camera (AOS-QPRI) for the first one, and the shadowgraph method with a high-speed digital camera (Phantom v611) for the second test set. A controllable injection system supplies an air–fuel mixture that is controlled manually or automatically based on data about the mixture's partial pressure, which has already been calculated. In this study, a special ignition system has been designed and constructed to have a successful spark to ignite the unburnt mixture, where the timing of the spark, and the power delivered are all controlled.

Hydrogen, ammonia, methane, and air are injected into the combustion chamber synchronously using a four-way manifold with four solenoid valves, where the fuels can be blended according to the volume fractions of the fuel, in which ammonia is the main fuel that is blended with methane based on the mole fraction of ammonia (X_{NH_3}). A control board was used to operate solenoid valves and regulate, control, and measure ignition power. Besides, it controls and measures the initial pressure, temperature, and heating system. All experiments were conducted at an initial temperature of 298 K. The accuracy of the pressure transducer (Rosemount), and thermocouple were ±0.1 kPa, and ±5 K, respectively.

It is essential to perform an uncertainty analysis of the laminar burning velocity. Each experiment was carried out 2–5 times to check the errors. The overall uncertainty (ΔS_L) was calculated using the approach suggested by Moffat et al. [60] and used by others such as Dai et al. [61]. It can be calculated as, $\Delta S_L = \sqrt{(B_R)^2 + \left(\frac{tS_R}{\sqrt{N}}\right)^2}$, where B_R is the total bias uncertainty that can be analyzed according to the method used by Lhuillier et al. [57] for estimate the bias for initial temperature, pressure, equation ratios, extrapolation, bouncy, and radiation; which can be expressed as,

$$B_R = (\Delta S_L)_T^2 + (\Delta S_L)_P^2 + (\Delta S_L)_\phi^2 + (\Delta S_L)_{Extrapolation}^2 + (\Delta S_L)_{Bouncy}^2 + (\Delta S_L)_{Radiation}^2$$

Additionally, S_R is the standard deviation of N repeated measurement, and t is the Student's multiplier for 95% confidence; where $S_R = \sqrt{\frac{\sum_{i=1}^{N}(X_i - \bar{X})^2}{N-1}}$. The overall experimental uncertainties of S_L were evaluated as ±0.7–9.0 cm/s.

Different equations were proposed to estimate the pressure and temperature dependencies on the laminar burning velocity since LBV has a correlation with (P_i/P_0) and (T_i/T_0). A simple power-low equation was suggested by Matghalchi et al. [62] as shown in Equation

$$S_L = S_{L,0}\left(\frac{P_i}{P_0}\right)^{\beta}\left(\frac{T_i}{T_0}\right)^{\alpha} \quad (1)$$

where $S_{L,0}$ is the laminar burning velocity at the reference temperature and pressure, and the pressure exponent (β) is a function of individual burning velocities at each pressure; therefore, uncertainty can be estimated with the error propagation rule according to [63]. Linear regression in logarithmic coordinates used to estimate the pressure exponent, assuming pressure measurements with no uncertainty and considering the uncertainty in the dependent variable S_L, can be calculated as:

$$\Delta\beta = \frac{\left(\sum_i \left[\left(\ln\frac{P_i}{P_0} - \overline{\ln\frac{P_i}{P_0}}\right)\cdot\frac{\Delta S_L^{P_i}}{S_L^{P_i}}\right]^2\right)^{0.5}}{\sum_i \ln^2\frac{P_i}{P_0} - n\cdot\left(\overline{\ln\frac{P_i}{P_0}}\right)^2} \quad (2)$$

where n is the number of data points (3), $\Delta S_L^{P_i}$ is the uncertainty of the burning velocity at reference pressure (mentioned above), P_0 is the reference pressure (0.1 MPa), and $\overline{\ln\frac{P_i}{P_0}}$ is the mean logarithmic normalized pressure. The overall uncertainty of β is 0.03. Based on Eq. (1), the pressure exponent can be estimated according to the slope of the straight line for the LBV-P plotted on a log–log scale for each equivalence ratio.

It is possible to estimate the radius of a normal spherical, centrally ignited, outwardly propagating flame directly from the Schlieren photographs to measure the laminar burning velocity. Recorded data may be affected by two significant determinants. When the flame radius is less than 6 mm, the flame speed is influenced by ignition energy, but it is independent of ignition energy when the flame radius exceeds 6 mm [64]. In addition, the second determinant is the flame radius from which meaningful data may be taken. The chamber condiment effect can be ignored when the radius is less than 40 mm (about 0.3 times the radius of the wall [65]). In this study, the affected laminar flame propagation speed is calculated using a flame radius of 8–40 mm for the

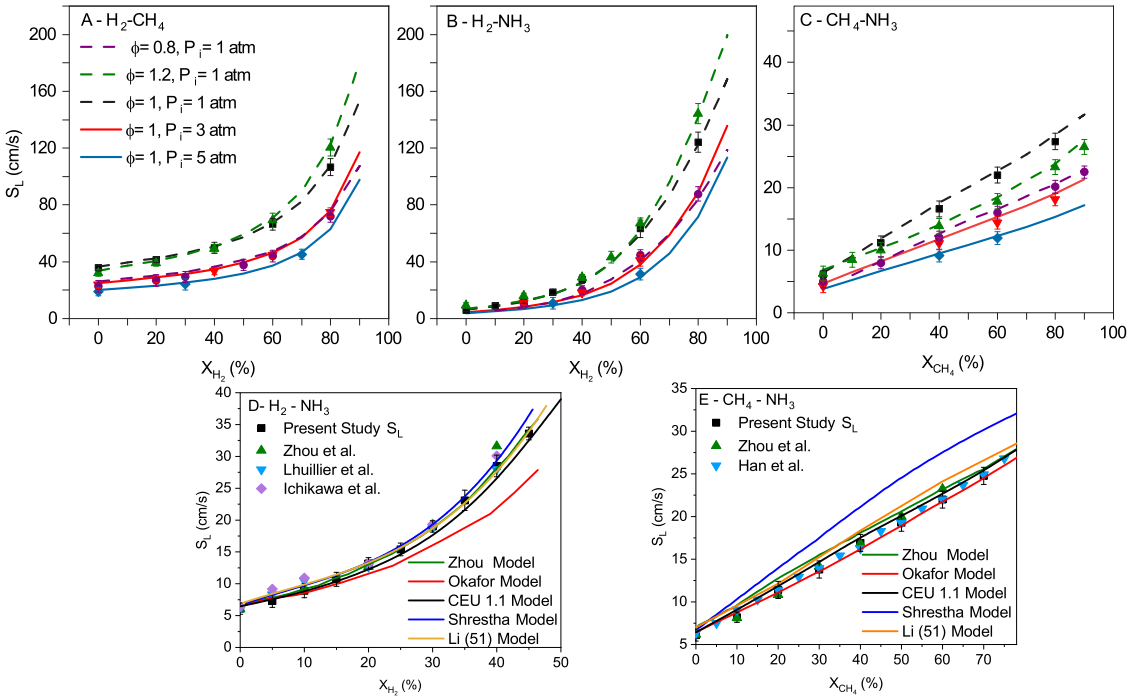

Fig. 2. Laminar burning velocity of dual fuel (A) H_2/CH_4, (B) H_2/NH_3, (C) CH_4/NH_3, (D) H_2/NH_3, and (E) CH_4/NH_3 - air flames versus fuel blends at different equivalence ratios and initial pressures at 298 K. The experimental results (scatters) compared with Wang et al. [54] model (line), while (D) and (E) results also validated with different models reported in the works of Okafor et al. [36], Shrestha et al. [55], Zhou et al. [56], and experimental data of Zhou et al. [56], Lhuillier et al. [57], Ichikawa et al. [58], Han et al. [59]. (For interpretation of the references to color in this figure legend, the reader is referred to the web version of this article.)

direct method of spherically centrally ignited outwardly propagating flame stretched flame speed, (S_n), which can be evaluated as follows:

$$S_n = \frac{dr_{sch}}{dt} \tag{3}$$

where r_{sch} is the radius of flame directly obtained from the Schlieren photos and t is the progress time. The spherically propagating flame is influenced by the effects of flame stretch. In the present study, the flame stretch rate, α, was evaluated using the following equation:

$$\alpha = \frac{1}{A_F}\frac{dA_F}{dt} = \frac{2}{r_{sch}}\frac{dr_{sch}}{dt} = 2\frac{S_n}{r} \tag{4}$$

where ($A_F = 4\pi r_{sch}^2$), is the area of flame front. Regarding the asymptotic analysis, the difference between S_s and S_n, can be considered to be proportional to the stretch rate, as shown by Eq. (5)

$$S_s - S_n = L_b \cdot \alpha \tag{5}$$

where L_b is the burned gas Markstein length. Thus, S_s can be calculated by the linear extrapolation of $\alpha \to 0$ (or $r_{sch} \to \infty$). S_L can then be calculated by $S_L = \frac{\rho_b}{\rho_u} \cdot S_s$ Here, ρ_b and ρ_u are the densities of burnt and unburnt mixture, respectively. Both densities are estimated from thermal equilibrium which is calculated by Chemkin-PRO.

The numerical simulation in this study is mostly based on Chemkin-Pro of the PREMIX module's flame speed freely propagating and equilibrium gas models, which correspond to one-dimensional and zero-dimensional flames, respectively. To achieve convergence (about 700 grid points), the chemical reaction kinetic mechanism, thermodynamic parameters, and transport parameter files must be regarded during the calculation process, and the adaptive gradient (GRAD) and curvature (CURV) were set to 0.02 for 10 cm domain.

3. Results and discussions

3.1. LBVs measurement of binary fuel mixtures

The determination of LBV of single and dual fuel mixtures at elevated pressure is validated using the constant volume method and compared with data from the literature [56–59] and findings from different kinetic models reported in the works of Okafor et al. [36], Shrestha et al. [55], Zhou et al. [56], and CEU-NH_3 1.1 [54]. It can be observed in Fig. 2 that the measured LBVs of NH_3/H_2 and H_2/CH_4 air mixtures semi-exponentially increase by increasing the hydrogen mixture at any initial pressure and equivalence ratios, while NH_3/CH_4/air mixtures linearly increase by increasing the methane mixture at any initial pressure and equivalence ratios. The measured results by different groups generally agree well with the lean and stoichiometric mixtures, while discrepancies appear on the rich side and higher hydrogen blends between these measured results. Therefore, it can be observed that the relative discrepancies on the rich side are quite apparent due to the low LBV values of the $NH_3/H_2/CH_4$/air mixtures.

As can be observed, the calculated LBVs for dual-fuel air flames are in excellent agreement with most of the published data. In addition, the present experimental data agree with the published data, especially in the stoichiometric and lean mixture. Okafor mechanism [36] predicts well the LBV for methane ammonia while underestimating the hydrogen–ammonia mixture. The Shrestha and Zhou mechanisms [34,56] overestimated on the rich side for hydrogen–ammonia mixture and overestimated in the estimation of LBVs of methane–ammonia dual blends, in general. In the case of the hydrogen–ammonia mixture, there is no subfigure to investigate the accuracy of mechanisms since most of these mechanisms are accurate in predictions of LBV.

The mechanism CEU-NH_3 1.1 [54] is selected as the optimum mechanism to be used in this study to predict the LBV of the ternary fuel mixture.

3.2. LBVs measurement of ternary fuel mixtures

The laminar burning velocity is the basic fundamental property of combustible mixtures and the key parameter in turbulent combustion. Based on the history of the flame radius in the large-scale combustion chamber, the S_L of $NH_3/H_2/CH_4$ air mixtures are extracted using a

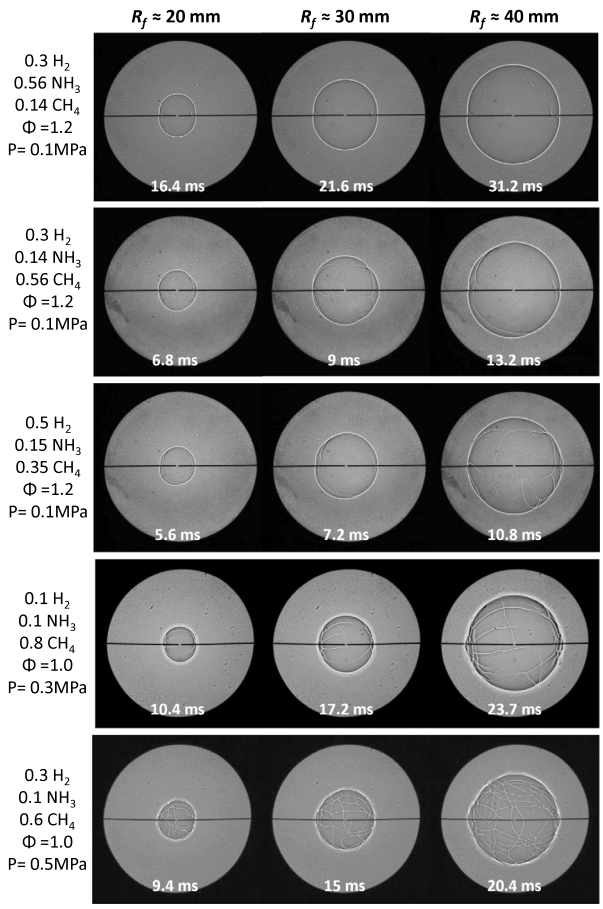

Fig. 3. Schlieren images of flame propagation for $0.3H_2$-$0.56NH_3$-$0.14CH_4$, $0.3H_2$-$0.14NH_3$-$0.56CH_4$, and $0.5H_2$-$0.15NH_3$-$0.35CH_4$ air flames at equivalence ratios of 1.2, initial pressure of 1 atm and initial temperature of 298 K.

linear approach. Fig. 3 shows a sequence of frames of an expanding spherical flame of a different ternary fuel–air mixture and equivalence ratios as an illustration of flame propagation. The Schlieren flame pictures clearly illustrate a circle whose diameter continues to expand over time. An expanding flame that develops from the center of the combustion chamber after a successful ignition may be smooth or have a few cracks on the surface of the flame. The disturbance during the ignition discharge process or spark electrodes is the major cause of these cracks. The next stage is the quasi-steady flame propagation stage, in which the flame expands outwards in a spherical smooth condition. In this stage, the flame is mostly dependent on the chemical reaction kinetics in the reaction zone. As mentioned previously, the experimental data are also used to obtain the laminar flame speed and hence the laminar burning velocity at this stage of propagation. The flame surface morphologies at different blending ratios seem different when the flame expands to a larger radius. The flame surface within the glass window remains smooth and indicates that there is no visible change in operating conditions. The flame surface is no longer as smooth for the stoichiometric ratio, and the initial cracks lose their natural appearance to grow and weakly divide. When the flame spreads to a larger radius for the working condition with a rich equivalent, the surface cracks initially continue to split before a cellular structure develops progressively. Furthermore, there is no obvious difference in the morphologies of the flames when the ammonia percentage is 30%–70%.

As the ammonia blend was reduced, the flame front surface progressively recovered spherical expansion, while the front surface became clearer and the flame stability increased. Increasing the hydrogen blend increases the flame propagation and makes it more stable as shown in Fig. 3. Increasing the initial pressure increases the elapsed time to reach a certain flame radius, i.e., with an increase in initial pressure, the flame propagation decreases. The laminar flame thickness decreases due to increased hydrogen blend because hydrogen has a higher diffusivity and flame speed than other fuels. This means the hydrogen molecules can mix and react with the air more quickly, resulting in a thinner flame. Furthermore, hydrogen has a higher flame temperature and a wider flammability range, contributing to the decrease in flame thickness. Overall, hydrogen's increased reactivity and combustion characteristics lead to a thinner laminar flame when blended with other fuels; this leads to instabilities in the flame front, causing it to become wrinkled or turbulent. Elevated pressures also contribute to flame wrinkling since the flame becomes more sensitive to instabilities due to increased heat release rates and changes in the fluid dynamics of the combustion process. Orange chemiluminescence; according to Hayakawa et al. [7], was generated by the NH_2 band spectrum and the superheated H_2O vapor spectrum for the combustion of ammonia. As the equivalence ratio increases, NH_2 levels increase, and orange chemiluminescence becomes more noticeable. The structure of the lean mixture flame became jellyfish-like as the flame radius increased. At $\phi = 0.8$, the unstretched laminar burning velocity is quite low. As a result, buoyancy is significantly influenced, particularly in this condition, and the flame structure varies as a result. At the beginning of propagation for higher ammonia blends, the center of the spherical flame was near the spark gap. As a result of buoyancy, the center of the spherical flame shifted upward in the combustion chamber. The size of the spherical flame decreased as the initial pressure of the mixture increased. It is possible to conclude that when the initial pressure of the mixture increases, the flame speed decreases.

High pressure is essential for the combustion characteristics that take place in most industrial applications. Because of this, it is essential to conduct research on the characteristics of fuel under pressures that are higher than those in the atmosphere.

Fig. 4 shows a ternary plot of the log-scale of the theoretical laminar burning velocity of $NH_3/H_2/CH_4$ air flames for different equivalence ratios and initial pressure at 298 K, calculated using CEU-NH_3 1.1 [54]. Increasing the hydrogen blend increases the LBV at any equivalence ratio or initial pressure. While LBV decreases with increased initial pressure and ammonia blend at any stoichiometry, a similar trend of LBV for single and dual fuel occurred in ternary fuel mixtures, where the maximum value tends to be on the slightly rich side. LBV for pure ammonia under higher pressure could not be estimated due to the buoyancy effect because LBV is very low in these conditions. When hydrogen and ammonia blend less than 55%, the measured LBVs in this area in the ternary plot (ammonia blend 0%–50%, hydrogen 0%–60%, and methane 0%–60%) show good agreement with pure methane–air mixtures, indicating that ternary fuel is a suitable alternative to methane in industrial applications. At elevated pressures, the same trend repeated with an increase of hydrogen blend. The most significant parameter of the decreasing trend of LBV with initial pressure is the increase in the density of the unburnt mixture. Instead of LBV, the mass flux (laminar burning flux) $f = \rho_u \times S_L = \rho_b \times S_S$, is the critical factor that is used to quantify the rate of flame propagation, where it increases with increased initial pressure. Even if the reaction rate increases as pressure increases, the LBV still decreases with pressure as a result of higher values of the unburned mixture density. The flame must physically move through and heat a stronger upstream.

It can be seen in Fig. 5 that 10% H_2 will apply a decrease of LBV of 33% is observed with an increase in pressure to 0.3 MPa, while LBV decreases by 45% when the initial pressure increases to 0.5 MPa compared to atmospheric conditions. It can be seen that increasing the equivalence ratio will decrease the effect of the initial pressure decrease for higher ammonia blends. In contrast, for low ammonia blends (less than 15%), the decrease in LBV increases with an increased equivalence ratio. This average decrease will not be affected by increasing hydrogen

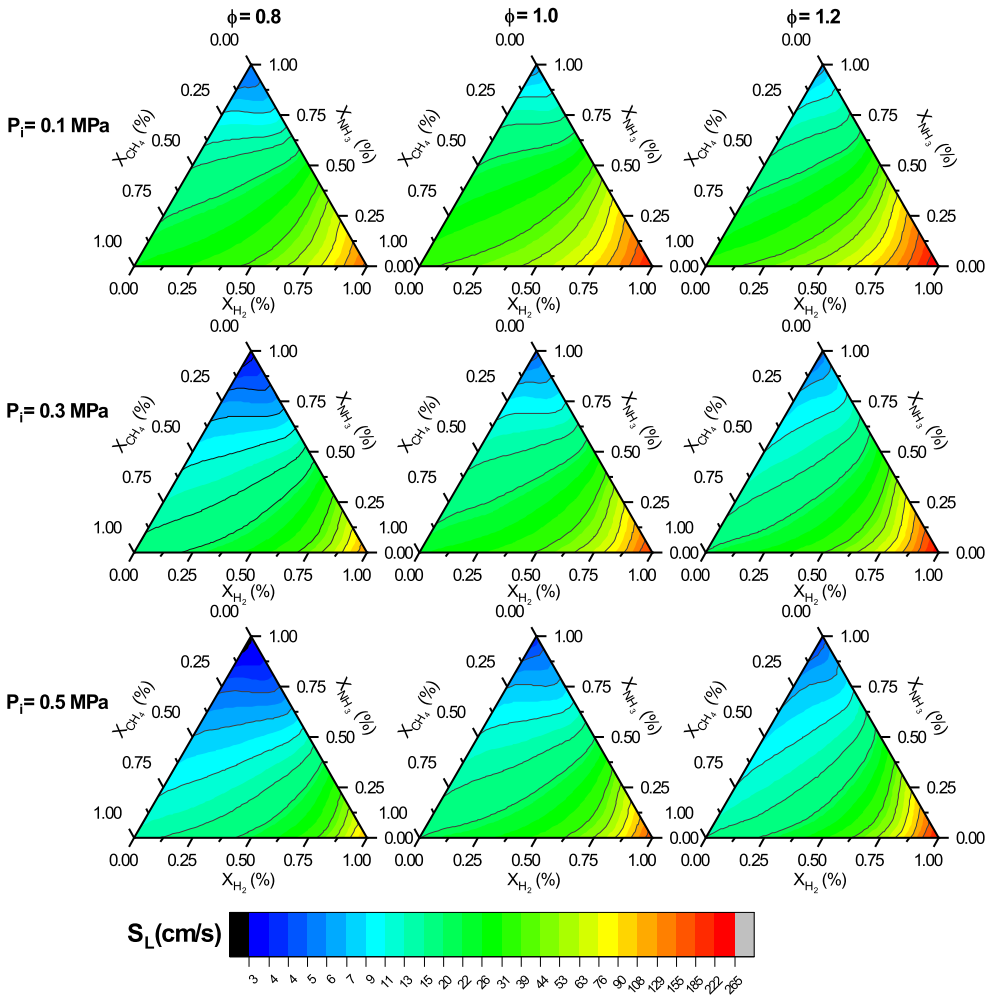

Fig. 4. Ternary plot of log-scale of the laminar burning velocity of $H_2/NH_3/CH_4$ air flames for different equivalence ratios and initial pressure at and 298 K, calculated using CEU-NH_3 1.1 [54].

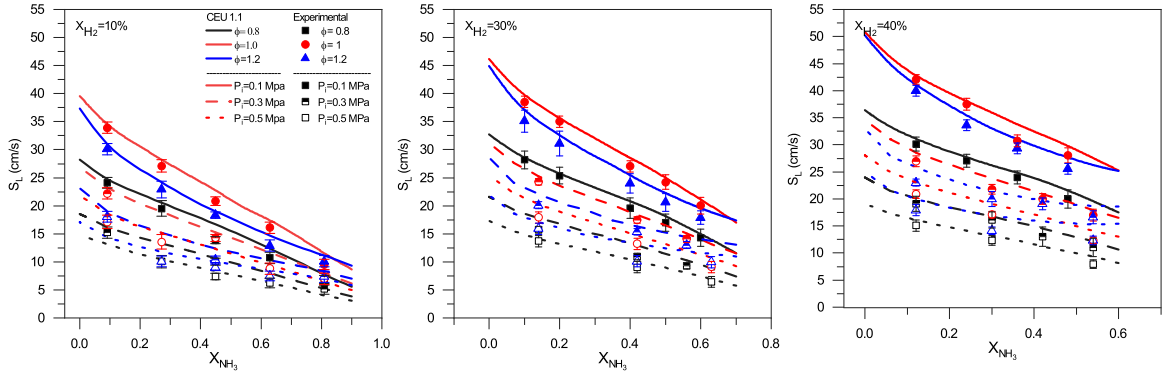

Fig. 5. Measured and simulated [54] laminar burning velocity of $H_2/NH_3/CH_4$ air flames at different initial pressure for (a) 10% H_2, (b) 30% H_2, and (c) 40% H_2 at different equivalence ratios and initial pressure at initial temperature of 298 K.

from 10% to 40%. It can also be noticed that CEU-NH_3 1.1 was under-predicted in atmospheric pressure and well-predicted in higher pressure. The decrease in LBV with an increase in initial pressure is due to the increase in density of the unburned mixture; moreover, increased initial pressure increases the heat release rate for all conditions due to decreases in thermal conductivity and increases in density. Under elevated pressures, $H + O_2 = O + OH$ and $H + CH_3(+M) = CH_4(+M)$ play significant roles, despite their importance decreasing with pressure. The increased sensitivity of inhibiting reactions $2CH_3(+M) = C_2H_6(+M)$ and $CH_4 + NH_2 = CH_3 + NH_3$ under elevated pressure implies that ignition is more sensitive to interactions between NH_3 and hydrocarbon species. Table 2 shows the calculated value of the pressure exponent from the experimental data, where increasing the ammonia blend decreases the pressure exponent at any pressure ratio or ϕ, while it increases with increasing hydrogen blends. There was a moderate increase in the values of pressure exponent from lean to stoichiometric conditions, and then two trends appeared in the table. The first observation occurs with a higher ammonia blend, which increases with the pressure exponent.

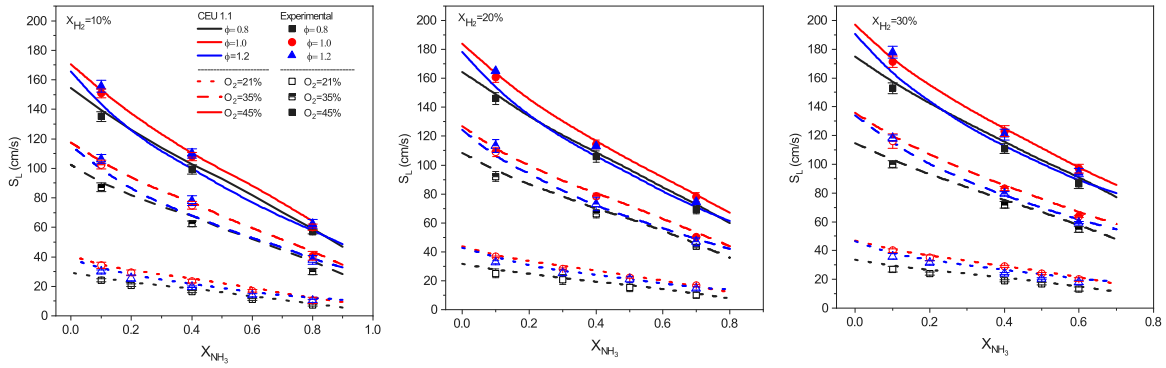

Fig. 6. Measured and simulated [54] laminar burning velocity of $H_2/NH_3/CH_4$ air flames at different oxygen enrichment ratios for (a) 10% H_2, (b) 20% H_2, and (c) 30% H_2 at different equivalence ratios and oxygen enrichment at initial pressure of 0.1 MPa and an initial temperature of 298 K.

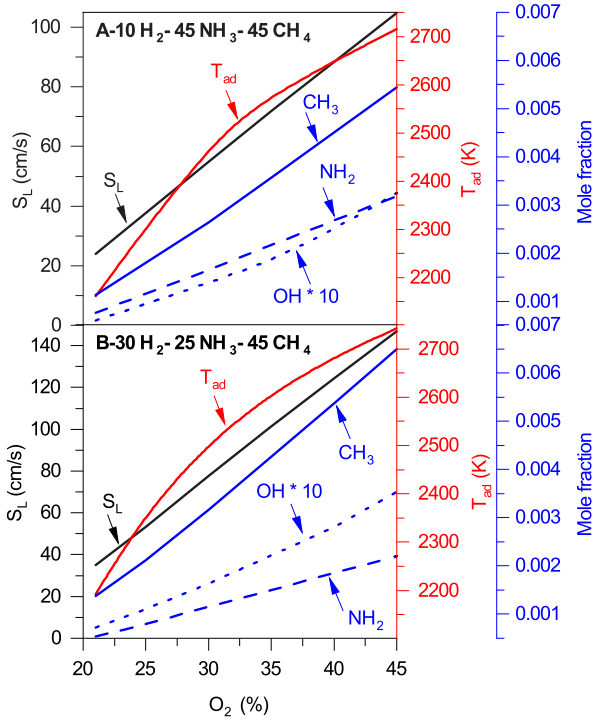

Fig. 7. Simulated adiabatic flame temperature, laminar burning velocity, and mole fractions of key radicals with different oxygen contents using CEU-NH_3 1.1 Mech. [54] for (A) 10 H_2 – 45NH_3 – 45 CH_4 and (B) 30 H_2 – 25NH_3 – 45 CH_4 air flames at equivalence ratio of 1, an initial pressure of 0.1 MPa and an initial temperature of 298 K.

Table 2
Pressure exponents at different equivalence ratios and fuel blends.

NH_3/CH_4	Equivalence ratio (ϕ)				
	0.8	0.9	1	1.1	1.2
For 10% H_2					
90/0	−0.379	−0.337	−0.290	−0.265	−0.255
72/18	−0.395	−0.375	−0.365	−0.390	−0.467
45/45	−0.425	−0.394	−0.359	−0.362	−0.369
18/72	−0.411	−0.390	−0.379	−0.396	−0.438
0	−0.397	−0.382	−0.379	−0.404	−0.463
For 30% H_2					
70/0	−0.423	−0.388	−0.334	−0.296	−0.278
56/14	−0.390	−0.370	−0.368	−0.382	−0.435
35/35	−0.426	−0.401	−0.391	−0.381	−0.382
14/56	−0.405	−0.391	−0.386	−0.393	−0.431
0//70	−0.391	−0.378	−0.374	−0.388	−0.444
For 40% H_2					
60/0	−0.467	−0.435	−0.369	−0.326	−0.305
48/12	−0.393	−0.364	−0.363	−0.373	−0.441
30/30	−0.429	−0.407	−0.386	−0.377	−0.391
12/48	−0.406	−0.387	−0.382	−0.389	−0.433
0/60	−0.386	−0.374	−0.370	−0.385	−0.442

In contrast, the mixture with higher methane shows that the pressure exponent decreases up to f ϕ 1.2 for this range of data.

Fig. 6 shows the measured and simulated LBV of NH_3/H_2 /CH_4/air flames for 10%–30% H_2 at different equivalence ratios (0.8,1 and 1.2), and oxygen enrichment (21%, 35%, and 45%) at an initial pressure of 0.1 MPa and an initial temperature of 298 K. The results show that LBV increases approximately four times in magnitude from air conditions to maximum oxygen content (45%) conditions due to oxygen enrichment. Ternary fuel is consumed using an abstraction reaction, specifically OH. For a higher ammonia mixture, NH_2 will be formed from the abstraction reaction and NH will be formed after reacting with H under lean conditions. While N_2H_2 produced by self-combination is more important in the rich side mixture. Furthermore, oxygen enrichment will enhance the promoting reaction (H + O_2 = O + OH) which is the most important high-temperature chain branching reaction. CH_3 follows the same methane decomposition trend and increases with increasing oxygen concentration.

Fig. 7 shows simulated adiabatic flame temperature and mole fractions of the OH radical with different oxygen enrichments at atmospheric pressure and temperature and $\phi = 1.0$ using CEU-NH_3 1.1. [54]. This provides a better understanding of the effect of oxygen enrichment on the LBV of the ternary fuel mixture. It can be noticed that increasing oxygen enrichment greatly increases the adiabatic flame temperature from 2150 K under the air condition to 2720 K under the maximum oxygen content condition, as shown in Fig. 7-A, which agrees with Law et al. [6]. Thus, the thermal effect of oxygen enrichment plays a dominant role in increasing the laminar burning velocity of ternary fuel. This is similar to those seen in the oxygen enrichment of hydrocarbon fuels. However, the mole fractions of the OH radical in the ternary fuel flames also continue to increase with increasing concentration of oxygen, demonstrating that the higher oxygen content improves the reactivity of the mixture and accelerates the propagation of the laminar flame. It can be noticed from Fig. 7-B that increasing the hydrogen blend increases LBV and T_{ad} and since the ammonia blend decreases with the constant methane blend, NH_2 decreases, but still has the same trend of increasing with an increase in oxygen concentration. Oxygen addition increases LBV due to the increasing OH radicals, which lead to consuming more in H radicals through the most sensitive reactions H + O_2 = O + OH, on the positive side and +CH_3(+M) = CH_4(+M), H + OH + M = H_2O +M, and H + O_2(+M) = HO_2(+M) on the negative side. While increases in ammonia blends promote some of the most

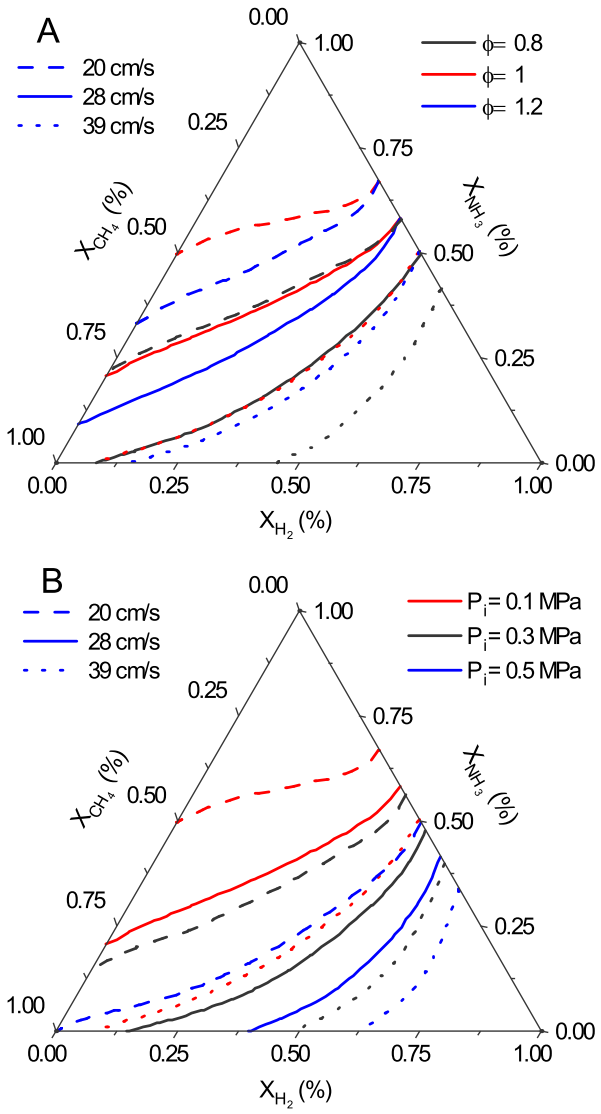

Fig. 8. Simulated laminar burning velocity [54] of $H_2/NH_3/CH_4$ air flames for constant laminar burning velocity 20, 28, 39 cm/s (A) at different equivalence ratios at initial pressure of 0.1 MPa; (B) at different initial pressures, with equivalence ratio of 1 and initial temperature of 298 K.

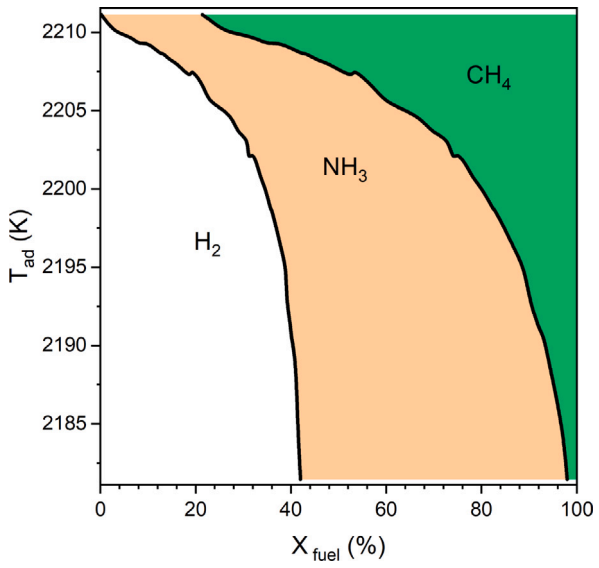

Fig. 9. Simulated adiabatic flame temperature [54] of $H_2/NH_3/CH_4$ air flames for constant laminar burning velocity 28 cm/s at an equivalence ratio of 1.0, an initial pressure of 0.1 MPa and an initial temperature of 298 K.

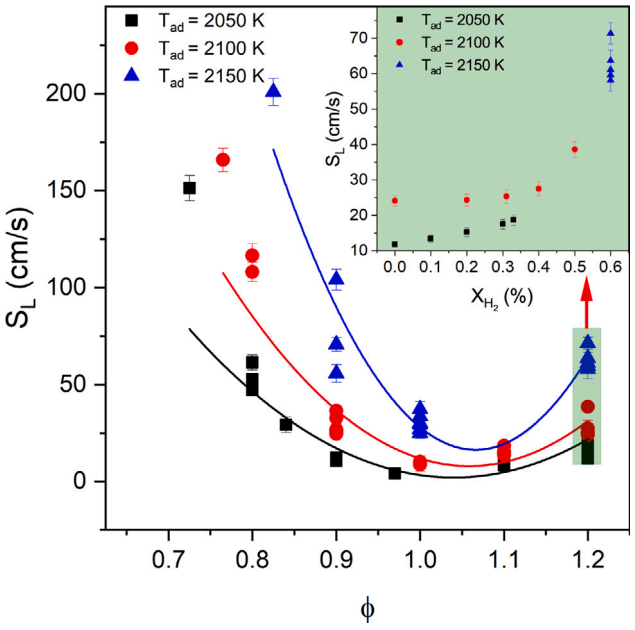

Fig. 10. Experimental laminar burning velocity of $H_2/NH_3/CH_4$ air flames for constant adiabatic flame temperature at different equivalence ratios, with initial pressure of 0.1 MPa and an initial temperature of 298 K.

significant chain-breaking reactions of NH_2 + NO = NNH + OH and NH_2 + NH = N_2H_2 + H, leading to increases in NH_2, hence, decreases both T_{ad} and S_L, alongside the three-body termination reactions of CH_3 to CH_4 generated C_2H_i; the formed N_2H_i then reacted to NNH and N_2.

Fig. 8 shows the simulated LBV [54] of $NH_3/H_2/CH_4$/air flames for constant laminar burning velocity (20, 28, and 39 cm/s) at different equivalence ratios, an initial pressure of 0.1 MPa and an initial temperature of 298 K. Since LBV is maximized near stoichiometry; the mixture at $\phi = 1$ at any constant LBV will tend to the upper side of the ternary plot, which means that the mixture has a larger ammonia mixture and fewer hydrogen and methane. It can be noticed that maintaining constant LBV is required to control the blending of the ternary fuel increasing the hydrogen blend from 0% to 40% to have a constant LBV of 28 cm/s required to increase the ammonia blend from 21% to 56% and reducing the methane blend from 79% to 0% as shown in Figs. 8 and 9. Fig. 8-B shows the effect of initial pressure on the laminar burning velocity for the ternary fuel–air mixture, where increasing initial pressure will decrease the LBV, thus maintaining the LBV constant, which is required to increase hydrogen. Furthermore, increasing LBV shifts the blend towards the right side of the ternary plot, where the mixture has more hydrogen, and methane, while having fewer ammonia concentrations. It can also be shown in Fig. 9 that adiabatic flame temperature increases with increasing methane concentration. On the contrary, both the ammonia and hydrogen concentrations are decreased, which means that the mixture tends to the left side in the ternary plot. An increase in the temperature of the adiabatic flame occurs when the density ratio increases, which maintains the LBV constant.

As can be seen from the experimental results in Fig. 10, for constant T_{ad}, laminar burning velocity decreases with increasing equivalence ratios and is minimized at slightly rich about 1.05, and then starts

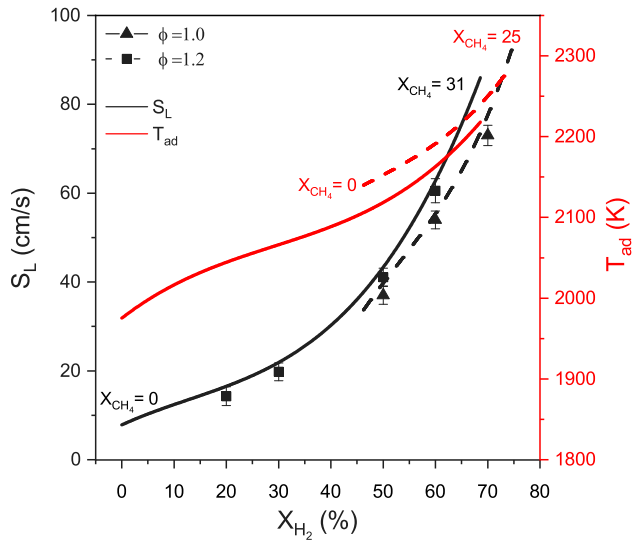

Fig. 11. Experimental and simulated laminar burning velocity and simulated adiabatic flame temperature of $H_2/NH_3/CH_4$ air flames for constant density ratio = 7.2 at equivalence ratios of 1 and 1.2, with an initial pressure of 0.1 MPa and an initial temperature of 298 K.

increasing again on the rich side. This is due to the increasing density ratio. Furthermore, increases in T_{ad} will increase LBV at higher concentrations of hydrogen and methane and fewer concentrations of ammonia. Besides, LBV and T_{ad} generally increase with increasing hydrogen blend, as shown in the sub-figure. Adiabatic flame temperature for each fuel is different, and the equivalence ratio has more impact compared with the initial pressure, where pure ammonia and hydrogen have T_{ad} of 2050 K at $\phi = 0.79$, while $\phi = 0.84$ for methane.

Fig. 11 shows the experimental and simulated laminar burning velocity and the simulated adiabatic flame temperature of $H_2/NH_3/CH_4$ air flames for a constant density ratio of 7.2 with an equivalence ratio of 1, and 1.2, an initial pressure of 0.1 MPa, and an initial temperature of 298 K. As can be observed from Fig. 11, the measured LBVs of the ternary fuel mixture are affected by hydrogen enrichment and the equivalence ratio since the constant density line semi-perpendicular on LBV and T_{ad} lines on the ternary plot. Therefore, increasing the blend of hydrogen and methane will increase LBV and T_{ad}, while the ammonia blend decreases. Sharp increment in LBV when hydrogen blends exceed 50%.

3.3. Sensitivity analyses of H_2 NH_3-CH_4/air flames

Fig. 12 illustrates normalized sensitivity coefficients in the forecast of S_L of NH_3/CH_4 with different blending ratios. As shown in Fig. 12, the small molecule-dominated N-consuming pathway was promoted, boosting the total reaction rate, whereas N_2H_i chemistry was moderately inhibited. According to the CH_4-NH_3 chemistry from the literature, the CH_3O chemistry was ignored, and the CH_3 reacted instantly with O to form CH_2O [48]. Researchers evaluated more comprehensive C/N interaction reactions; slight amounts in CH_4-NH_3 co-oxidation were evaluated numerically and experimentally [50,66], though since CEU-NH_3 1.1 tends to rely on the Konnov mechanism [32] have a satisfactory precision estimate to provide further important species forecasts, including such HCN in CH_4-NH_3 flames. Furthermore, the CH_4-NH_3 chemistries indirectly interacted with estimating the laminar flame speed by having a relatively similar active radical pool of H, O, and OH. Due to the consumption of H radicals, the most sensitive reactions with positive signs were H + O_2 = O + OH, HCO(+M) = H + CO(+M), and NH_2 + NO = NNH + OH. The most sensitive reactions with negative signs were H + CH_3(+M) = CH_4(+M), NH_2 + O = HNO + H, and H + O_2(+M) = HO_2(+M). H_2/CO chemistries were reported to still dominate the oxidation at high temperatures. The CH_3 and HCO radicals had a significant influence on NH_3/CH_4 flame speeds, but at high NH_3 concentrations, the NH_2 + NO and NH_2 + NH– dominated the flux direction of N- elements and the flame speed. Furthermore, the high uncertainty of N_2H_i chemistries were evaluated as key factors of flame speed, in addition to some of the most significant chain breaking reactions of NH_2 + NO = NNH + OH and NH_2 + NH = N_2H_2 + H, as H radicals can be generated by reactions and the pathway of N_2H_2 → NNH → N_2. While the lower speed of flame propagation, even in high ammonia blends, three-body termination reactions of CH_3 to CH_4 generated C_2H_i; the formed N_2H_i then reacted to NNH and N_2. According to Fig. 12-A, for lean mixtures, OH + H_2 = H + OH and CO + OH = CO + H dominate on the positive side, while H + O_2(+M) = HO_2(+M) dominates on the negative side, which implies that the lean side is almost dominated by H_2 chemistry. The rich side showed NH_2 + NH = N_2H_2 + H for the first time. While Furthermore, Fig. 12-B illustrates that CEU-NH_3 1.1 contained the reaction NH_2 + NH = N_2H_3 from Pagsberg et al. [67] Due to the general enhancement of OH radicals in the radical pool with the admitting of H_2, this reaction plays chain propagating and terminating purposes in the production of H and provides a high sensitivity in the rich mixture for NH_3-H_2-air flame, the NH_3 oxidation is promoted by NH + OH = NH_2 + H_2O, which also has an important effect on S_L. Due to the completely different reaction pathway of N_2H_3, if the combined reaction of NH_2 and NH generates N_2H_3 instead of N_2H_2, the production of H radicals is inhibited. The impact of NH_3 chemistry on S_L is considerably inhibited in the NH_3/CH_4/air flame, such as NH_2 + NH = N_2H_2 + H. Because CH_4 competes strongly with active radicals, more active radicals will react with CH_4 to complete the oxidation process. HCO + M = H + CO + M has the highest positive sensitivity coefficient, showing that CO chemistry dominates the increasing laminar flame speed of ternary fuel/air mixtures. It can be noticed that CO chemistry is the most dominant, followed by the H_2 chemistry. NO chemistry only has a slight positive effect on S_L. Furthermore, Ammonia blending with fuels having a high reactivity may not be a suitable option for inhibiting the NO production, while the increment of NO emissions because hydrogen and methane promote NH_2 to NO, and then inhibited the NO reduction by H_2. Experimental result consistent with the inferences has been found by Wargadalam et al. [68].

Fig. 12-D shows the pressure effect on 30 H_2 – 35NH_3 – 35 CH_4 fuel blending mixture at different initial pressures at equivalence ratios of 1. H + CH_3(+M) = CH_4(+M) and NH_2 + O = HNO + H, and H + O_2 = O + OH are the key boosting and inhibitory reactions for LBV, where increasing initial pressure promote H + O_2(+M) = HO_2(+M) which increases the consumption of H radicles. Moreover, 2OH = O + H_2O, NH_3 + OH = NH_2 + H_2O, and CH_3OH (+M) = CH_3 + OH (+M) participate only at elevated pressure while HCO + OH = CO + H_2O, NH_2 + HO_2 = NH_3 + O_2, and NH_2 + NH = N_2H_3 having less contribution at elevated pressure, and therefore LBV decreases.

Fig. 13 demonstrates the sensitivity of NO concentration concerning the most important reactions. Like LBV sensitivity, chain branching reactions such as H + O_2 = O + OH have the most positive effect on NO production in the mixtures, and with ammonia content increases, this reaction becomes more important for constant hydrogen content, while the minimum amount of ammonia will promote this reaction at constant methane contents. Kohansal et al. [69]mentioned that the production of NO or N_2 in ammonia chemistry highly depends on NH_i radicals' preference to react with NO or O/H radicals. The reaction of NH_i with the pool of radicals leads to the formation of HNO through NH_2 + OH = HNO + H and NH + O = HNO + H, while the production of N_2H_2 formed through NH_2 + NH = N_2H + H. Kohansal et al. [69] reported that the concentration of NO has a rising-falling behavior with ammonia mole fraction for CH_4-NH_3-air flames, and this behavior occurred in 40% ammonia blends, which is related to the concentration of amine (NH and NH_2) and active radicals. The production of No

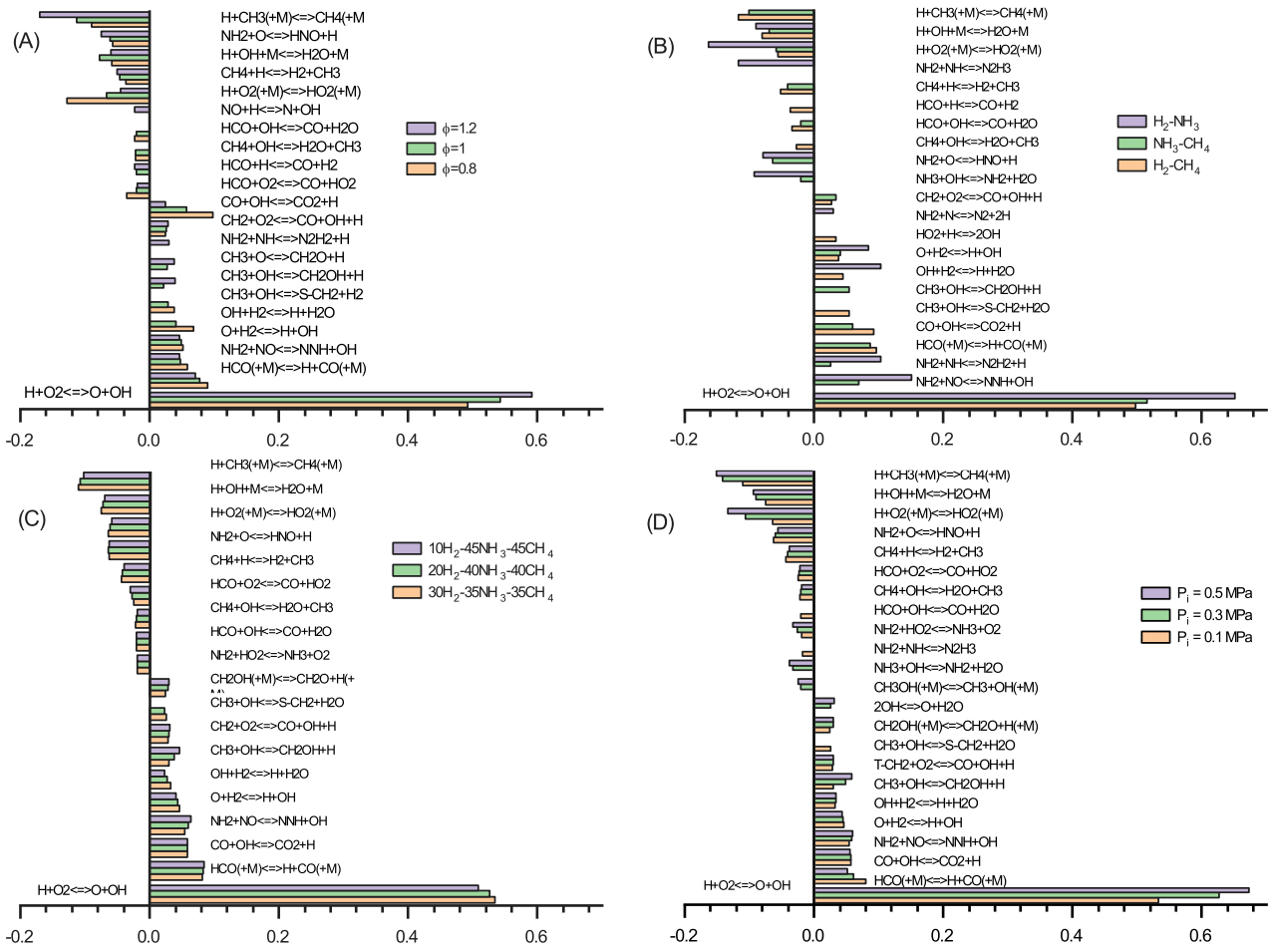

Fig. 12. Sensitivity coefficient of the laminar burning velocity concerning the most rate-limiting reactions using [54] at an initial pressure of 0.1 MPa and an initial temperature of 298 K, (A) 40 H_2 – 30NH_3 – 30 CH_4 fuel blending mixture at different equivalence ratios, (B) dual fuel blending at equivalence ratios of 1, and (C) different ternary fuel blending mixture at equivalence ratios of 1, (D) 30 H_2 – 35NH_3 – 35 CH_4 fuel blending mixture at different initial pressure at equivalence ratios of 1.

increases for low NH_3 content more than pure ammonia because of the high number of H, O, and OH radicals, and subsequently, NO production decreases because of the lowering concentration of active radicals. N + NO = N_2 + O is the most important reaction to reduce NO mainly produced by the second important inhibiting reaction NO_2 + H = NH + NO. Furthermore, the reduction in NO increases when the ammonia content increases due to NH_2 + NO = N_2 + H_2O.

4. Conclusions

In view of the fossil fuel insufficiency and air pollution, this study explores the potential of a $NH_3/H_2/CH_4$ ternary fuel mixture that can be considered a suitable alternative for conventional fuels in industrial applications. This study uses expanding spherical flames and Schlieren imaging techniques in a constant volume chamber at elevated initial pressure and oxygen enrichment to evaluate a key combustion characteristic: Laminar Burning Velocity (LBV) of different $NH_3/H_2/CH_4$ blends. On the other hand, numerical analysis was performed using CHEMKIN Pro software. When hydrogen and ammonia blend about 10%–50% at elevated mixture pressures, the measured LBV values show good agreement with pure methane–air mixtures, indicating that ternary fuel is a suitable alternative for methane in industrial applications. Experiments with different blends of ternary fuel mixtures were controlled by adjusting these three variables: concentration, equivalence ratio, oxygen concentrations, and initial pressure. The most important findings from the current investigations are as follows:

1. At any conditions investigated, the maximum laminar burning velocity achieves its maximum value close to an equivalence ratio of 1.05. Increasing the initial pressure causes a decrease in the laminar burning velocity. Oxygen enrichment causes an increase in LBV. That tendency is the same as that of dual-fuel and single-hydrocarbon fuels. A decrease of 33% for LBV is observed at 10% H2 when the initial pressure increases to 0.3 MPa, while at 0.5 MPa, the LBV decreases by 45% compared to atmospheric conditions.
2. LBV increases with increasing hydrogen blends and decreases with increasing ammonia blends under any conditions. Because of the presence of nitroxyl (HNO) radicals, LBV decreases by 12% and 16% under stoichiometric conditions when NH_3 blend increases 10%–20%, respectively.
3. Increasing oxygen content improves the reactivity of the mixture and accelerates LBV, due to increasing OH, NH_2, and CH_3 radicals in the ternary fuel flames. An increase in LBV of approximately four times and Adiabatic Flame Temperature (T_{ad}) increases by 550 K when oxygen content increases to (45%).
4. Maintaining a constant LBV value requires controlling the blending ratio of the ternary fuels. Constant LBV at 28 cm/s requires an increase in the hydrogen blend from 0% to 40%, and at the same time, ammonia increases from 21% to 56%, while the methane blend decreases from 79% to 0%. Raising LBV values shifted the mixture towards the higher hydrogen and methane and fewer ammonia concentrations in the ternary plot.
5. When T_{ad} is kept constant, LBV decreases with increases in the equivalence ratio, approaching a minimum at a slightly rich

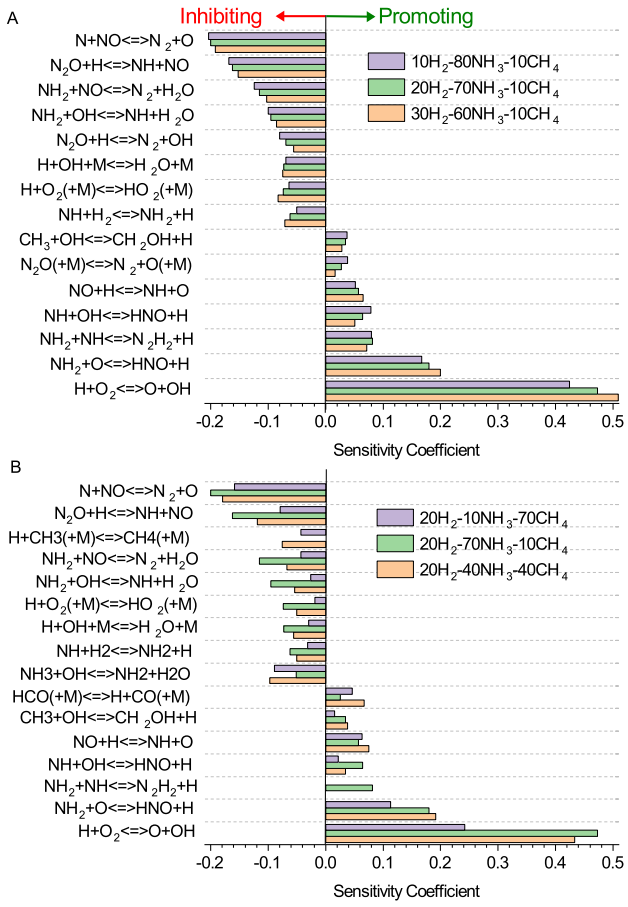

Fig. 13. Sensitivity coefficient of NO concentration concerning the most rate-limiting reactions at the point of maximum NO concentration at equivalence ratios of 1, with an initial pressure of 0.1 MPa and an initial temperature of 298 K. (A) 10% methane blend for different ammonia blends, and (B) 20% hydrogen blend and different ammonia blends.

equivalence ratio of roughly 1.05 before increasing again on the rich side, a reverse trend of the density ratio. Furthermore, regardless of the initial conditions, increasing the hydrogen blend regularly increases LBV and T_{ad}. As the constant density line is perpendicular to the LBV and T_{ad} lines in the ternary plot, the LBV and T_{ad} ratios increase with increasing hydrogen blend under any equivalence ratios. It makes the selection of an alternative ternary blending fuel more precise.

Declaration of competing interest

The authors declare that they have no known competing financial interests or personal relationships that could have appeared to influence the work reported in this paper.

Acknowledgments

This study is partially supported by the National Natural Science Foundation of China (No. 52076171), the Shaanxi Science and Technology Innovation Team, China (2021TD-22), also by the Major Science and Technology Projects of Inner Mongolia Autonomous Region, China (2021ZD0025), and the Science Center for Gas Turbine Project, China (P2022-A-II-006-001).

References

[1] Kobayashi Hideaki, Hayakawa Akihiro, Somarathne KD Kunkuma A, Okafor Ekenechukwu C. Science and technology of ammonia combustion. Proc Combust Inst 2019;37(1):109–33.

[2] Elbaz Ayman M, Wang Shixing, Guiberti Thibault F, Roberts William L. Review on the recent advances on ammonia combustion from the fundamentals to the applications. Fuel Commun 2022;100053.

[3] Valera-Medina Agustin, Xiao Hua, Owen-Jones Martin, David William IF, Bowen PJ. Ammonia for power. Prog Energy Combust Sci 2018;69:63–102.

[4] Chai Wai Siong, Bao Yulei, Jin Pengfei, Tang Guang, Zhou Lei. A review on ammonia, ammonia-hydrogen and ammonia-methane fuels. Renew Sustain Energy Rev 2021;147:111254.

[5] Yapicioglu Arda, Dincer Ibrahim. A review on clean ammonia as a potential fuel for power generators. Renew Sustain Energy Rev 2019;103:96–108.

[6] Law Chung K. Combustion physics. Cambridge University Press; 2010.

[7] Hayakawa Akihiro, Goto Takashi, Mimoto Rentaro, Kudo Taku, Kobayashi Hideaki. NO formation/reduction mechanisms of ammonia/air premixed flames at various equivalence ratios and pressures. Mech Eng J 2015;2(1):14–00402.

[8] Vandooren Jacques, Bian J, Van Tiggelen PJ. Comparison of experimental and calculated structures of an ammonia nitric oxide flame. Importance of the NH2+ NO reaction. Combust Flame 1994;98(4):402–10.

[9] Lewis Bernard, Von Elbe Guenther. Combustion, flames and explosions of gases. Elsevier; 2012.

[10] Michalsky Ronald, Parman Bryon J, Amanor-Boadu Vincent, Pfromm Peter H. Solar thermochemical production of ammonia from water, air and sunlight: Thermodynamic and economic analyses. Energy 2012;42(1):251–60.

[11] Ritter James A, Ebner Armin D, Wang Jun, Zidan Ragaiy. Implementing a hydrogen economy. Mater Today 2003;6(9):18–23.

[12] Okanishi T, Okura K, Srifa A, Muroyama H, Matsui T, Kishimoto M, Saito M, Iwai H, Yoshida H, Saito M, et al. Comparative study of Ammonia-fueled solid oxide fuel cell systems. Fuel Cells 2017;17(3):383–90.

[13] Miyazaki Kazunari, Okanishi Takeou, Muroyama Hiroki, Matsui Toshiaki, Eguchi Koichi. Development of Ni–Ba (Zr, Y) O3 cermet anodes for direct ammonia-fueled solid oxide fuel cells. J Power Sources 2017;365:148–54.

[14] Chiong Meng-Choung, Chong Cheng Tung, Ng Jo-Han, Mashruk Syed, Chong William Woei Fong, Samiran Nor Afzanizam, Mong Guo Ren, Valera-Medina Agustin. Advancements of combustion technologies in the ammonia-fuelled engines. Energy Convers Manage 2021;244:114460.

[15] Rocha Rodolfo C, Costa Mário, Bai Xue-Song. Combustion and emission characteristics of ammonia under conditions relevant to modern gas turbines. Combust Sci Technol 2021;193(14):2514–33.

[16] Kurien Caneon, Mittal Mayank. Review on the production and utilization of green ammonia as an alternate fuel in dual-fuel compression ignition engines. Energy Convers Manage 2022;251:114990.

[17] Boretti A. Novel dual fuel diesel-ammonia combustion system in advanced TDI engines. Int J Hydrogen Energy 2017;42(10):7071–6.

[18] Yasiry Ahmed Sh, Shahad Haroun AK. An experimental study of the effect of hydrogen blending on burning velocity of LPG at elevated pressure. Int J Hydrogen Energy 2016;41(42):19269–77. http://dx.doi.org/10.1016/j.ijhydene.2016.08.097.

[19] Cai Xiao, Wang Jinhua, Zhang Weijie, Xie Yongliang, Zhang Meng, Huang Zuohua. Effects of oxygen enrichment on laminar burning velocities and Markstein lengths of CH4/O2/N2 flames at elevated pressures. Fuel 2016;184:466–73. http://dx.doi.org/10.1016/j.fuel.2016.07.011.

[20] Hu Erjiang, Li Xiaotian, Meng Xin, Chen Yizhen, Cheng Yu, Xie Yongliang, Huang Zuohua. Laminar flame speeds and ignition delay times of methane–air mixtures at elevated temperatures and pressures. Fuel 2015;158:1–10. http://dx.doi.org/10.1016/j.fuel.2015.05.010.

[21] Han Wang, Dai Peng, Gou Xiaolong, Chen Zheng. A review of laminar flame speeds of hydrogen and syngas measured from propagating spherical flames. Appl Energy Combust Sci 2020;1:100008.

[22] Konnov Alexander A, Mohammad Akram, Kishore Velamati Ratna, Kim Nam Il, Prathap Chockalingam, Kumar Sudarshan. A comprehensive review of measurements and data analysis of laminar burning velocities for various fuel+ air mixtures. Prog Energy Combust Sci 2018;68:197–267.

[23] Hu Erjiang, Huang Zuohua, He Jiajia, Miao Haiyan. Experimental and numerical study on laminar burning velocities and flame instabilities of hydrogen–air mixtures at elevated pressures and temperatures. Int J Hydrog Energy 2009;34(20):8741–55.

[24] Wang Shixing, Wang Zhihua, Elbaz Ayman M, Han Xinlu, He Yong, Costa Mário, Konnov Alexander A, Roberts William L. Experimental study and kinetic analysis of the laminar burning velocity of NH3/syngas/air, NH3/CO/air and NH3/H2/air premixed flames at elevated pressures. Combust Flame 2020;221:270–87.

[25] Varghese Robin John, Kolekar Harshal, Kishore V Ratna, Kumar Sudarshan. Measurement of laminar burning velocities of methane-air mixtures simultaneously at elevated pressures and elevated temperatures. Fuel 2019;257:116120.

[26] Qin Xiao, Kobayashi Hideaki, Niioka Takashi. Laminar burning velocity of hydrogen–air premixed flames at elevated pressure. Exp Therm Fluid Sci 2000;21(1–3):58–63.

[27] Bradley D, Lawes M, Liu Kexin, Verhelst Sebastian, Woolley R. Laminar burning velocities of lean hydrogen–air mixtures at pressures up to 1.0 MPa. Combust Flame 2007;149(1–2):162–72.

[28] Kanoshima Ryuhei, Hayakawa Akihiro, Kudo Takahiro, Okafor Ekenechukwu C, Colson Sophie, Ichikawa Akinori, Kudo Taku, Kobayashi Hideaki. Effects of initial mixture temperature and pressure on laminar burning velocity and markstein length of ammonia/air premixed laminar flames. Fuel 2022;310:122149.
[29] Yin Geyuan, Li Jinglun, Zhou Meng, Li Jiaxing, Wang Chaojun, Hu Erjiang, Huang Zuohua. Experimental and kinetic study on laminar flame speeds of ammonia/dimethyl ether/air under high temperature and elevated pressure. Combust Flame 2022;238:111915.
[30] Berwal Pragya, Kumar Sudarshan, et al. Laminar burning velocity measurement of CH4/H2/NH3-air premixed flames at high mixture temperatures. Fuel 2023;331:125809.
[31] Ó Conaire Marcus, Curran Henry J, Simmie John M, Pitz William J, Westbrook Charles K. A comprehensive modeling study of hydrogen oxidation. Int J Chem Kinet 2004;36(11):603–22.
[32] Konnov Alexander A. Remaining uncertainties in the kinetic mechanism of hydrogen combustion. Combust Flame 2008;152(4):507–28.
[33] Li Rui, Konnov Alexander A, He Guoqiang, Qin Fei, Zhang Duo. Chemical mechanism development and reduction for combustion of NH3/H2/CH4 mixtures. Fuel 2019;257:116059.
[34] Shrestha Krishna Prasad, Lhuillier Charles, Barbosa Amanda Alves, Brequigny Pierre, Contino Francesco, Mounaïm-Rousselle Christine, Seidel Lars, Mauss Fabian. An experimental and modeling study of ammonia with enriched oxygen content and ammonia/hydrogen laminar flame speed at elevated pressure and temperature. Proc Combust Inst 2021;38(2):2163–74.
[35] Okafor Ekenechukwu Chijioke, Naito Yuji, Colson Sophie, Ichikawa Akinori, Kudo Taku, Hayakawa Akihiro, Kobayashi Hideaki. Measurement and modelling of the laminar burning velocity of methane-ammonia-air flames at high pressures using a reduced reaction mechanism. Combust Flame 2019;204:162–75.
[36] Okafor Ekenechukwu C, Naito Yuji, Colson Sophie, Ichikawa Akinori, Kudo Taku, Hayakawa Akihiro, Kobayashi Hideaki. Experimental and numerical study of the laminar burning velocity of CH4–NH3–air premixed flames. Combust Flame 2018;187:185–98.
[37] Mitu Maria, Razus Domnina, Schroeder Volkmar. Laminar burning velocities of hydrogen-blended methane–air and natural gas–air mixtures, calculated from the early stage of p (t) records in a spherical vessel. Energies 2021;14(22):7556.
[38] Di Sarli V, Di Benedetto A. Laminar burning velocity of hydrogen–methane/air premixed flames. Int J Hydrogen Energy 2007;32(5):637–46.
[39] Pessina V, Berni F, Fontanesi S, Stagni A, Mehl M. Laminar flame speed correlations of ammonia/hydrogen mixtures at high pressure and temperature for combustion modeling applications. Int J Hydrogen Energy 2022;47(61):25780–94.
[40] Amirante Riccardo, Distaso Elia, Tamburrano Paolo, Reitz Rolf D. Laminar flame speed correlations for methane, ethane, propane and their mixtures, and natural gas and gasoline for spark-ignition engine simulations. Int J Engine Res 2017;18(9):951–70.
[41] Ali SM, Varunkumar S. Effect of burner diameter and diluents on the extinction strain rate of syngas-air non-premixed Tsuji-type flames. Int J Hydrogen Energy 2020;45(15):9113–27.
[42] Benaissa Sabrina, Adouane Belkacem, Ali Syed Mughees, Mohammad Akram. Effect of hydrogen addition on the combustion characteristics of premixed biogas/hydrogen-air mixtures. Int J Hydrogen Energy 2021;46(35):18661–77.
[43] Mashruk Syed, Vigueras-Zuniga Marco Osvaldo, Tejeda-del Cueto Maria-Elena, Xiao Hua, Yu Chunkan, Maas Ulrich, Valera-Medina Agustin. Combustion features of CH4/NH3/H2 ternary blends. Int J Hydrogen Energy 2022;47(70):30315–27.
[44] Benaissa Sabrina, Adouane Belkacem, Ali Syed Mughees, Rashwan Sherif S, Aouachria Z. Investigation on combustion characteristics and emissions of biogas/hydrogen blends in gas turbine combustors. Therm Sci Eng Prog 2022;27:101178.
[45] Berwal Pragya, Khandelwal Bhupendra, Kumar Sudarshan. Effect of ammonia addition on laminar burning velocity of CH4/H2 premixed flames at high pressure and temperature conditions. Int J Hydrogen Energy 2023.
[46] Berwal Pragya, Kumar Sudarshan, Khandelwal Bhupendra. Laminar burning velocity measurement of NH3/H2/CH4 fuel blends at elevated temperature and pressure. In: AIAA SCITECH 2023 forum. 2023, p. 0201.
[47] Bayramoğlu Kubilay, Bahlekeh Abdullah, Masera Kemal. Numerical investigation of the hydrogen, ammonia and methane fuel blends on the combustion emissions and performance. Int J Hydrogen Energy 2023.
[48] Somarathne Kapuruge Don Kunkuma Amila, Hatakeyama Sotaro, Hayakawa Akihiro, Kobayashi Hideaki. Numerical study of a low emission gas turbine like combustor for turbulent ammonia/air premixed swirl flames with a secondary air injection at high pressure. Int J Hydrogen Energy 2017;42(44):27388–99.
[49] Miller James A, Smooke Mitchell D, Green Robert M, Kee Robert J. Kinetic modeling of the oxidation of ammonia in flames. Combust Sci Technol 1983;34(1–6):149–76.
[50] Glarborg Peter, Miller James A, Ruscic Branko, Klippenstein Stephen J. Modeling nitrogen chemistry in combustion. Prog Energy Combust Sci 2018;67:31–68.
[51] Valera-Medina Agustin, Gutesa M, Xiao H, Pugh D, Giles A, Goktepe B, Marsh R, Bowen P. Premixed ammonia/hydrogen swirl combustion under rich fuel conditions for gas turbines operation. Int J Hydrogen Energy 2019;44(16):8615–26.
[52] Khateeb Abdulrahman A, Guiberti Thibault F, Wang Guoqing, Boyette Wesley R, Younes Mourad, Jamal Aqil, Roberts William L. Stability limits and NO emissions of premixed swirl ammonia-air flames enriched with hydrogen or methane at elevated pressures. Int J Hydrogen Energy 2021;46(21):11969–81.
[53] Tang Guang, Jin Pengfei, Bao Yulei, Chai Wai Siong, Zhou Lei. Experimental investigation of premixed combustion limits of hydrogen and methane additives in ammonia. Int J Hydrogen Energy 2021;46(39):20765–76.
[54] Wang Shixing, Wang Zhihua, Chen Chenlin, Elbaz Ayman M, Sun Zhiwei, Roberts William L. Applying heat flux method to laminar burning velocity measurements of NH3/CH4/air at elevated pressures and kinetic modeling study. Combust Flame 2022;236:111788.
[55] Shrestha Krishna P, Seidel Lars, Zeuch Thomas, Mauss Fabian. Detailed kinetic mechanism for the oxidation of ammonia including the formation and reduction of nitrogen oxides. Energy Fuels 2018;32(10):10202–17.
[56] Zhou Shangkun, Cui Baochong, Yang Wenjun, Tan Houzhang, Wang Jinhua, Dai Hongchao, Li Liangyu, ur Rahman Zia, Wang Xiaoxiao, Deng Shuanghui, et al. An experimental and kinetic modeling study on NH3/air, NH3/H2/air, NH3/CO/air, and NH3/CH4/air premixed laminar flames at elevated temperature. Combust Flame 2023;248:112536.
[57] Lhuillier Charles, Brequigny Pierre, Lamoureux Nathalie, Contino Francesco, Mounaïm-Rousselle Christine. Experimental investigation on laminar burning velocities of ammonia/hydrogen/air mixtures at elevated temperatures. Fuel 2020;263:116653.
[58] Ichikawa Akinori, Hayakawa Akihiro, Kitagawa Yuichi, Somarathne KD Kunkuma Amila, Kudo Taku, Kobayashi Hideaki. Laminar burning velocity and markstein length of ammonia/hydrogen/air premixed flames at elevated pressures. Int J Hydrogen Energy 2015;40(30):9570–8.
[59] Han Xinlu, Wang Zhihua, Costa Mario, Sun Zhiwei, He Yong, Cen Kefa. Experimental and kinetic modeling study of laminar burning velocities of NH3/air, NH3/H2/air, NH3/CO/air and NH3/CH4/air premixed flames. Combust Flame 2019;206:214–26.
[60] Moffat Robert J. Describing the uncertainties in experimental results. Exp Therm Fluid Sci 1988;1(1):3–17.
[61] Dai Hongchao, Wang Jinhua, Cai Xiao, Su Shouguo, Zhao Haoran, Huang Zuohua. Measurement and scaling of turbulent burning velocity of ammonia/methane/air propagating spherical flames at elevated pressure. Combust Flame 2022;242:112183.
[62] Metghalchi Mohamad, Keck James C. Burning velocities of mixtures of air with methanol, isooctane, and indolene at high pressure and temperature. Combust Flame 1982;48:191–210.
[63] Goswami M, Bastiaans RJM, De Goey LPH, Konnov AA. Experimental and modelling study of the effect of elevated pressure on ethane and propane flames. Fuel 2016;166:410–8.
[64] Bradley Derek, Gaskell Philip H, Gu Xiao-Jun. Burning velocities, Markstein lengths, and flame quenching for spherical methane-air flames: a computational study. Combust Flame 1996;104(1–2):176–98.
[65] Burke Michael P, Chen Zheng, Ju Yiguang, Dryer Frederick L. Effect of cylindrical confinement on the determination of laminar flame speeds using outwardly propagating flames. Combust Flame 2009;156(4):771–9.
[66] Tian Zhenyu, Li Yuyang, Zhang Lidong, Glarborg Peter, Qi Fei. An experimental and kinetic modeling study of premixed NH3/CH4/O2/Ar flames at low pressure. Combust Flame 2009;156(7):1413–26.
[67] Pagsberg Palle Bjø rn, Eriksen J, Christensen HC. Pulse radiolysis of gaseous ammonia-oxygen mixtures. J Phys Chem 1979;83(5):582–90.
[68] Wargadalam VJ, Löffler G, Winter F, Hofbauer H. Homogeneous formation of NO and N2O from the oxidation of HCN and NH3 at 600–1000 °c. Combust Flame 2000;120(4):465–78.
[69] Kohansal MohammadReza, Kiani Mehrdad, Masoumi Soheil, Nourinejad Soroush, Ashjaee Mehdi, Houshfar Ehsan. Experimental and numerical investigation of NH3/CH4 mixture combustion properties under elevated initial pressure and temperature. Energy Fuels 2023;37(14):10681–96.